

THERMOSENSITIVE RESPONSE OF A FUNCTIONALLY GRADED CYLINDER WITH FRACTIONAL ORDER DERIVATIVE

Navneet Kumar LAMBA

Department of Mathematics, Shri Lemdeo Patil Mahavidyalaya, Mandhal, Nagpur, INDIA
E-mail: navneet19021984kumar@gmail.com

The present paper deals with thermal behaviour analysis of an axisymmetric functionally graded thermosensitive hollow cylinder. The system of coordinates are expressed in cylindrical-polar form. The heat conduction equation is of time-fractional order $0 < \alpha \leq 2$, subjected to the effect of internal heat generation. Convective boundary conditions are applied to inner and outer curved surfaces whereas heat dissipates following Newton's law of cooling. The lower surface is subjected to heat flux, whereas the upper surface is thermally insulated. Kirchhoff's transformation is used to remove the nonlinearity of the heat equation and further it is solved to find temperature and associated stresses by applying integral transformation method. For numerical analysis a ceramic-metal-based functionally graded material is considered and the obtained results of temperature distribution and associated stresses are presented graphically.

Key words: time fractional, thick hollow cylinder, thermal stresses, internal heat generation, FGMs, thermosensitive.

1. Introduction

Fractional thermoelasticity involves the heat conduction equation of fractional order and the differential operator shows memory effects. At present, the theory of fractional calculus have wide applications in applied engineering and sciences like robotics, bioengineering, geology, etc. First in 2005, Povstenko [1] introduced the heat conduction equation of fractional order and described corresponding thermal stresses. Then after he developed and modify various new models based on the fraction theory of thermoelasticity as reflected in [2, 3, 4, 5, 6]. Thermosensitive bodies are those homogeneous or piecewise-homogeneous bodies whose thermo-physical characteristics are temperature dependent. Popovich *et al.* [7, 8, 9, 10, 11, 12] studied numerical-analytical solutions of various thermoelastic problems with non-steady heat-conduction in homogeneous thermosensitive bodies. All these bodies were subjected to prescribed temperature or heat flux on the boundaries which were completely linearized by using the Kirchhoff variable transformation technique.

Functionally graded materials (FGMs) are materials having compositions of a microstructure, or porosity across the volume of the material. Also this materials are adaptable as heat-resistant materials and have attractive application in furnace lines, space structures, fusion reactors and electronics component packaging. FGMs are new versions of composite materials that are microscopically inhomogeneous in unique characterization. Guo and Noda [13] determined the thermal stresses for a thin FGM cylindrical shell with effect of thermal shock. Cheng and Batra [14, 15] established an exact deflection relationship between different functionally graded plate theories and that of an equivalent homogenous Kirchhoff plate. Other related studies by assuming cylindrical bodies with different boundary conditions are described in [16, 17, 18, 19, 20, 21, 22].

During solidification or sublimation or melting most thermally sensitive materials release significant amounts of energy. Also, during the heating process these materials absorb energy and transfer energy to the environment in the cooling process. Therefore, an analysis of time fractional thermo-sensitivity is very important in various cylindrical structures which are made of FGMs. Recently, Thakare and Warbhe [23] studied the time fractional order thermoelastic problem of a thermally sensitive functionally graded thick hollow cylinder with the effect of internal heat source. Thakre *et al.* [24] solved a two dimensional

thermoelastic problem and determined temperature and associated stresses for a non-homogeneous thick hollow cylinder within the context of fractional order theory.

The article presented here is related to the extension of our own work [23, 24] by assuming the time fractional governing temperature and spatial variable dependent heat conduction problem for a thick functionally graded hollow cylinder with an internal heat source (geometry as shown in Fig.1). Except Poisson's ratio all the material properties are considered to be dependent on both temperature and spatial variable z . The heat conduction equation is solved by using integral transformation and by introducing Kirchhoff's variable transformation. The solution is obtained in the form of Bessel's and trigonometric functions.

2. Formulation of the problem

A functionally graded axisymmetric thermosensitive thick hollow cylinder is considered with internal heat generation of radius varying from $r = a$ to $r = b$ and thickness from $z = 0$ to $z = h$, occupying the space $D = \{(x, y, z) \in R^3 : 0 \leq z \leq h \text{ and } a \leq (x^2 + y^2)^{1/2} \leq b\}$ where $r = (x^2 + y^2)^{1/2}$.

The above thermoelastic problem is framed mathematically for a nonlocal Caputo type time fractional heat conduction equation of order α in case of FG thick hollow cylinder. The expression for Caputo type fractional derivative of function $f(t)$ is given as [6]

$$\frac{d^\alpha f(t)}{dt^\alpha} = \frac{1}{\Gamma(n-\alpha)} \int_0^t (t-\tau)^{n-\alpha-1} \frac{d^n f(\tau)}{d\tau^n} d\tau, \quad t > 0, \quad n-1 < \alpha < n, \quad (2.1)$$

with the following Laplace transform rule, where Caputo derivative needs the initial values of the function $f(t)$ and its corresponding integral derivatives of order $k = 1, 2, 3, \dots, n-1$

$$L\left\{\frac{d^\alpha f(t)}{dt^\alpha}\right\} = s^\alpha L\{\bar{f}(s)\} - \sum_{k=0}^{n-1} f^{(k)}(0^+) s^{\alpha-1-k}, \quad n-1 < \alpha < n, \quad (2.2)$$

in which s is the transform parameter and n is a positive integer.

2.1. Governing equation of temperature distribution function with boundaries

The time fractional governing temperature and spatial variable dependent heat conduction problem for a thick functionally graded hollow cylinder with an internal heat source is represented as

$$\begin{aligned} \frac{1}{r} \frac{\partial}{\partial r} \left(r k(z, T) \frac{\partial T}{\partial r} \right) + \frac{\partial}{\partial z} \left(k(z, T) \frac{\partial T}{\partial z} \right) + \\ + Q_0 \delta(r - r_0) \delta(z - z_0) \delta(t) = c(z, T) \frac{\partial^\alpha T}{\partial t^\alpha}, \end{aligned} \quad (2.3)$$

subjected to corresponding initial and boundary condition as

$$\left(k(z, T) \frac{\partial T}{\partial r} - \varepsilon_l (T - T_0) \right) \Big|_{r=a} = Q_l \delta(z - z_0) \delta(t); \quad 0 \leq z \leq h, \quad t > 0, \quad (2.4)$$

$$\left(k(z,T) \frac{\partial T}{\partial r} + \varepsilon_2 (T - T_0) \right) \Big|_{r=b} = Q_1 \delta(z - z_0) \delta(t); \quad 0 \leq z \leq h, \quad t > 0, \quad (2.5)$$

$$\left(k(z,T) \frac{\partial T}{\partial z} \right) \Big|_{z=0} = Q_2 \delta(r - r_0) \delta(t); \quad a \leq r \leq b, \quad t > 0, \quad (2.6)$$

$$\left(\frac{\partial T}{\partial z} \right) \Big|_{z=h} = 0; \quad a \leq r \leq b, \quad t > 0, \quad (2.7)$$

$$T = T_0, \quad \text{at} \quad t = 0, \quad 0 < \alpha \leq 2, \quad (2.8)$$

$$\frac{\partial T}{\partial t} = 0, \quad \text{at} \quad t = 0, \quad 1 < \alpha \leq 2 \quad (2.9)$$

where, $T(r, z, t)$ refers to temperature distribution at any time t , T_0 denotes the surrounding medium temperature, at $(r = r_0, z = z_0)$ the expression $Q_0 \delta(r - r_0) \delta(z - z_0) \delta(t)$ denotes the instantaneous point heat source of strength Q_0 . Further $Q_1 \delta(z - z_0) \delta(t)$ is the heat of the strength Q_1 at the point $(r = a, z = z_0)$ and $Q_2 \delta(r - r_0) \delta(t)$ is the heat of the strength Q_2 at $(r = b, z = z_0)$ and $(r = r_0, z = 0)$, respectively, $k(z, T)$ represents the thermal conductivity and $c(z, T)$ denotes specific heat capacity for the thick hollow cylinder, further $\varepsilon_1, \varepsilon_2$ denote the coefficient of heat transfer.

2.2. Thermal stresses and displacements expressions

Following Hata [25], the expression for strain-displacement and condition of equilibrium of the thick hollow cylinder is as follows

$$e_{rr} = \frac{\partial u}{\partial r}, \quad e_{\theta\theta} = \frac{u}{r}, \quad e_{zz} = \frac{\partial w}{\partial z}, \quad e_{rz} = \frac{1}{2} \left(\frac{\partial u}{\partial z} + \frac{\partial w}{\partial r} \right), \quad (2.10)$$

$$\frac{\partial \sigma_{rr}}{\partial r} + \frac{\partial \sigma_{rz}}{\partial z} + \frac{\sigma_{rr} - \sigma_{\theta\theta}}{r} = 0, \quad (2.11)$$

$$\frac{\partial \sigma_{rz}}{\partial r} + \frac{\partial \sigma_{zz}}{\partial z} + \frac{\sigma_{rz}}{r} = 0, \quad (2.12)$$

here u and w denote the displacement components along the radial and axial directions, respectively.

In the case of temperature dependent material properties the relationship between stress and strain functions are given as

$$\sigma_{rr} = 2G_0 z^\beta e^{\alpha T} e_{rr} + \lambda_0 z^\beta e^{\alpha T} e - \left(3\lambda_0 z^\beta e^{\alpha T} + 2\mu_0 z^\beta e^{\alpha T} \right) \alpha_0 z^\beta e^{\chi T} T, \quad (2.13)$$

$$\sigma_{\theta\theta} = 2G_0 z^\beta e^{\alpha T} e_{\theta\theta} + \lambda_0 z^\beta e^{\alpha T} e - \left(3\lambda_0 z^\beta e^{\alpha T} + 2\mu_0 z^\beta e^{\alpha T} \right) \alpha_0 z^\beta e^{\chi T} T, \quad (2.14)$$

$$\sigma_{zz} = 2G_0 z^\beta e^{\varpi T} e_{zz} + \lambda_0 z^\beta e^{\varpi T} e - \left(3\lambda_0 z^\beta e^{\varpi T} + 2\mu_0 z^\beta e^{\varpi T} \right) \alpha_0 z^\beta e^{\chi T} T, \quad (2.15)$$

$$\sigma_{rz} = 2G_0 z^\beta e^{\varpi T} e_{rz}, \quad (2.16)$$

here, $e = (e_{rr} + e_{\theta\theta} + e_{zz})$ and $e_{rr}, e_{\theta\theta}, e_{zz}$ denote the strain components, $G_0 z^\beta e^{\varpi T}$ stands for the shear modulus, $\mu_0 z^\beta e^{\varpi T}$ and $\lambda_0 z^\beta e^{\varpi T}$ are the Lamé's constants and the thermal expansion coefficient is represented by $\alpha_0 z^\beta e^{\chi T}$.

On substituting Eqs (2.13)-(2.16) in (2.11) and (2.12), the required equilibrium equations of displacements is

$$\begin{aligned} \Delta^2 u - \frac{u}{r^2} + \varpi \frac{\partial u}{\partial r} \frac{\partial T}{\partial r} + \frac{\lambda_0}{2G_0 \mu_0} \left(\frac{\partial \varepsilon}{\partial r} + \varepsilon \varpi \frac{\partial T}{\partial r} \right) + \frac{\partial^2 w}{\partial r \partial z} + \left(\frac{\partial u}{\partial z} + \frac{\partial w}{\partial r} \right) \left(\varpi \frac{\partial T}{\partial z} + \frac{\beta}{z} \right) + \\ - \alpha_0 \left(\frac{3\lambda_0}{2\mu_0} + 1 \right) z^\beta e^{\chi T} \frac{\partial T}{\partial r} (\varpi T + T + 1) = 0, \end{aligned} \quad (2.17)$$

$$\begin{aligned} \Delta^2 w + \frac{\partial^2 u}{\partial r \partial z} + \left(\frac{\partial u}{\partial z} + \frac{\partial w}{\partial r} \right) \left(\varpi \frac{\partial T}{\partial r} + \frac{1}{r} \right) + \left(\frac{\partial w}{\partial z} + \frac{\lambda_0 \varepsilon}{\mu_0} \right) \left(\varpi \frac{\partial T}{\partial z} + \frac{\beta}{z} \right) + \\ + \frac{\lambda_0}{2G_0 \mu_0} \frac{\partial \varepsilon}{\partial z} - \alpha_0 \left(\frac{3\lambda_0}{2\mu_0} + 1 \right) z^\beta e^{\chi T} \frac{\partial T}{\partial r} \varpi T = 0 \end{aligned} \quad (2.18)$$

where ∇^2 is given by

$$\nabla^2 = \frac{\partial^2}{\partial r^2} + \frac{1}{r} \frac{\partial}{\partial r} + \frac{\partial^2}{\partial z^2}. \quad (2.19)$$

Using the thermoelastic Goodier's displacement potential φ as well as Boussinesq harmonic functions ϕ and ψ with no body forces in cylindrical coordinates the solution of Eqs (2.13)-(2.16) is as follows

$$u = \frac{\partial \phi}{\partial r} + \frac{\partial \varphi}{\partial r} + z \frac{\partial \psi}{\partial r}, \quad (2.20)$$

$$w = \frac{\partial \phi}{\partial z} + \frac{\partial \varphi}{\partial z} + z \frac{\partial \psi}{\partial z} - (3 - 4\nu) \psi \quad (2.21)$$

where

$$\nabla^2 \varphi = K(T - T_0), \quad \nabla^2 \phi = 0, \quad \text{and} \quad \nabla^2 \psi = 0. \quad (2.22)$$

The coefficient of restraint is

$$K(z, t) = \frac{(1+\nu)}{(1-\nu)} \alpha_0 z^\beta e^{\chi T}.$$

For the sake of brevity, we take

$$-\int (\phi + z\psi) dz = M. \quad (2.23)$$

Now substituting Eq.(2.23) in (2.20) and (2.21), the harmonic functions ϕ and ψ are expressed in terms of Michell's function M as

$$u = \frac{\partial \phi}{\partial r} - \frac{\partial^2 M}{\partial r \partial z}, \quad (2.24)$$

$$w = \frac{\partial \phi}{\partial z} + 2(1-\nu) \nabla^2 M - \frac{\partial^2 M}{\partial z^2} \quad (2.25)$$

where

$$\nabla^2 \nabla^2 M = 0. \quad (2.26)$$

Further, the resultant stresses are obtained by substituting (2.24)-(2.25) in (2.13) to (2.16) as

$$\begin{aligned} \sigma_{rr} = z^\beta e^{\chi T} & \left\{ 2G_0 \frac{\partial}{\partial r} \left[\frac{\partial \phi}{\partial r} - \frac{\partial^2 M}{\partial r \partial z} \right] + \right. \\ & \left. + \lambda_0 \left[\nabla^2 \phi + (1-2\nu) \frac{\partial}{\partial z} (\nabla^2 M) \right] - (3\lambda_0 + 2\mu_0) \alpha_0 z^\beta e^{\chi T} T \right\}, \end{aligned} \quad (2.27)$$

$$\begin{aligned} \sigma_{\theta\theta} = z^\beta e^{\chi T} & \left\{ 2G_0 \frac{1}{r} \left[\frac{\partial \phi}{\partial r} - \frac{\partial^2 M}{\partial r \partial z} \right] + \right. \\ & \left. + \lambda_0 \left[\nabla^2 \phi + (1-2\nu) \frac{\partial}{\partial z} (\nabla^2 M) \right] - (3\lambda_0 + 2\mu(z)) \alpha_0 z^\beta e^{\chi T} T \right\}, \end{aligned} \quad (2.28)$$

$$\begin{aligned} \sigma_{zz} = z^\beta e^{\chi T} & \left\{ 2G_0 \frac{\partial}{\partial z} \left(\frac{\partial \phi}{\partial z} + 2(1-\nu) \nabla^2 M - \frac{\partial^2 M}{\partial z^2} \right) + \right. \\ & \left. + \lambda_0 \left[\nabla^2 \phi + (1-2\nu) \frac{\partial}{\partial z} (\nabla^2 M) \right] - (3\lambda_0 + 2\mu_0) \alpha_0 z^\beta e^{\chi T} T \right\}, \end{aligned} \quad (2.29)$$

$$\sigma_{rz} = z^\beta e^{\chi T} G_0 \left\{ \left[\frac{\partial}{\partial z} \left[\frac{\partial \phi}{\partial r} - \frac{\partial^2 M}{\partial r \partial z} \right] + \frac{\partial}{\partial r} \left(\frac{\partial \phi}{\partial z} + (1-2\nu) \nabla^2 M - \frac{\partial^2 M}{\partial z^2} \right) \right] \right\}. \quad (2.30)$$

Further, in traction free surface the following stress functions satisfy

$$\left. \begin{aligned} \sigma_{rr} = 0 & \quad \text{at} \quad r = a \quad \text{and} \quad r = b, \\ \sigma_{zz} = 0 & \quad \text{at} \quad z = 0 \quad \text{and} \quad z = h. \end{aligned} \right\} \quad (2.31)$$

Modeling of the functionally graded thermal sensitive hollow cylinder problem in the context of fractional theory with internal heat is presented above.

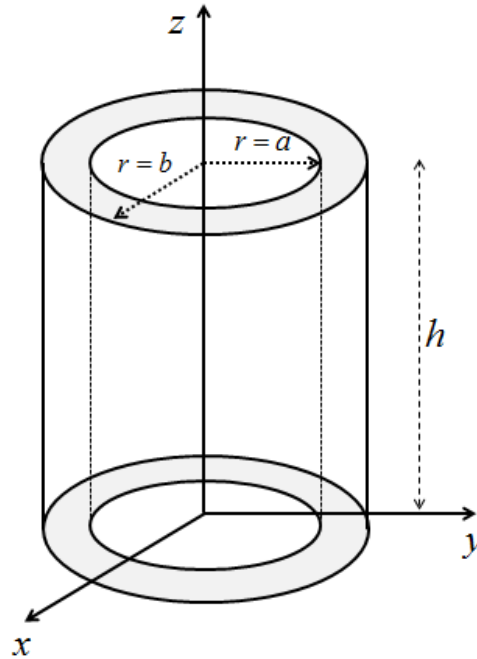


Fig.1. Geometry of the nonhomogeneous hollow cylinder.

3. Solution of the problem

3.1. Solution of the heat conduction problem

Following Noda [26], we have

$$k(z, T) = z^\beta k(T), \quad c(z, T) = z^\beta k(T). \quad (3.1)$$

Further, following Popovych *et al.* [3, 4, 5, 10, 13, 17] by introducing the Kirchhoff's variable

$$\Theta = \int_{T_0}^T k(z, T) dT. \quad (3.2)$$

Next, the material is considered with simple thermal nonlinearity

$$C(T) / k(T) = 1. \quad (3.3)$$

By taking account of Eqs (3.1), (3.2) and (3.3), Eq.(2.3) is rewritten as

$$\left(\frac{\partial^2 \Theta}{\partial r^2} + \frac{1}{r} \frac{\partial \Theta}{\partial r} \right) + \frac{\partial^2 \Theta}{\partial z^2} + Q_0 \delta(r - r_0) \delta(z - z_0) \delta(t) = \frac{\partial^\alpha \Theta}{\partial t^\alpha}. \quad (3.4)$$

Corresponding boundary and initial conditions are

$$\left(\frac{\partial \Theta}{\partial r} - \varepsilon_1 \Theta \right) \Big|_{r=a} = Q_1 \delta(z - z_0) \delta(t); \quad 0 \leq z \leq h, \quad t > 0, \quad (3.5)$$

$$\left(\frac{\partial \Theta}{\partial r} + \varepsilon_2 \Theta \right) \Big|_{r=b} = Q_1 \delta(z - z_0) \delta(t); \quad 0 \leq z \leq h, \quad t > 0, \quad (3.6)$$

$$\left(\frac{\partial \Theta}{\partial z} \right) \Big|_{z=0} = Q_2 \delta(r - r_0) \delta(t); \quad a \leq r \leq b, \quad t > 0, \quad (3.7)$$

$$\left(\frac{\partial \Theta}{\partial z} \right) \Big|_{z=h} = 0; \quad a \leq r \leq b, \quad t > 0, \quad (3.8)$$

$$\Theta = 0, \quad \text{at} \quad t = 0, \quad 0 < \alpha \leq 2, \quad (3.9)$$

$$\frac{\partial \Theta}{\partial t} = 0, \quad \text{at} \quad t = 0, \quad 1 < \alpha \leq 2. \quad (3.10)$$

Applying the Laplace transform to Eq.(3.4) and using boundary conditions (3.9)-(3.10), one obtains

$$\left(\frac{\partial^2 \Theta^*}{\partial r^2} + \frac{1}{r} \frac{\partial \Theta^*}{\partial r} \right) + \frac{\partial^2 \Theta^*}{\partial z^2} + Q_0 \delta(r - r_0) \delta(z - z_0) = s^\alpha \Theta^*. \quad (3.11)$$

Corresponding boundary and initial conditions are,

$$\left(\frac{\partial \Theta^*}{\partial r} - \varepsilon_1 \Theta^* \right) \Big|_{r=a} = Q_1 \delta(z - z_0), \quad 0 \leq z \leq h, \quad t > 0, \quad (3.12)$$

$$\left(\frac{\partial \Theta^*}{\partial r} + \varepsilon_2 \Theta^* \right) \Big|_{r=b} = Q_1 \delta(z - z_0), \quad 0 \leq z \leq h, \quad t > 0, \quad (3.13)$$

$$\left(\frac{\partial \Theta^*}{\partial z} \right) \Big|_{z=0} = Q_2 \delta(r - r_0), \quad a \leq r \leq b, \quad t > 0, \quad (3.14)$$

$$\left. \left(\frac{\partial \Theta^*}{\partial z} \right) \right|_{z=h} = 0, \quad a \leq r \leq b, \quad t > 0. \quad (3.15)$$

Further, using the transform by Al-Hajri and Kalla [27] to solve Eq.(3.11) over the variable r , using transformed boundary condition (3.12) and (3.13) as

$$\begin{aligned} & (b\varepsilon_2 M(q_n b) Q_I - a\varepsilon_1 M(q_n a) Q_I) \delta(z - z_0) - q_n^2 \bar{\Theta}^* + \frac{\partial^2 \bar{\Theta}^*}{\partial z^2} + \\ & + Q_0 r_0 M(q_n r_0) \delta(z - z_0) = s^\alpha \bar{\Theta}^*, \end{aligned} \quad (3.16)$$

$$\left. \left(\frac{\partial \bar{\Theta}^*}{\partial z} \right) \right|_{z=0} = Q_2 r_0 M(q_n r_0), \quad a \leq r \leq b, \quad t > 0, \quad (3.17)$$

$$\left. \left(\frac{\partial \bar{\Theta}^*}{\partial z} \right) \right|_{z=h} = 0, \quad a \leq r \leq b, \quad t > 0 \quad (3.18)$$

where

$$M(q_n r) = [B(q_n a, -\varepsilon_1) + B(q_n b, \varepsilon_2)] J_0(q_n r) - [A(q_n a, -\varepsilon_1) + B(q_n b, \varepsilon_2)] Y_0(q_n r),$$

in which

$$A(q_n r, \varepsilon_{n1}) = \varepsilon_{n1} J_0(q_n r) + q_n J_0'(q_n r); \quad n_1 = 1, 2, \quad r = a, b,$$

$$B(q_n r, \varepsilon_{n1}) = \varepsilon_{n1} Y_0(q_n r) + q_n Y_0'(q_n r); \quad n_1 = 1, 2, \quad r = a, b$$

where the Bessel's functions of first and second kind are denoted by J_0 and Y_0 and q_n is the '+' roots of the following transcendental equation

$$B(q_n a, -\varepsilon_1) \times A(q_n a, \varepsilon_2) - A(q_n a, -\varepsilon_1) \times B(q_n a, \varepsilon_2) = 0.$$

Next, using the finite Fourier cosine transform to (3.16) over the variable z under transformed boundary (3.17) and (3.18), one obtains

$$\begin{aligned} & (b\varepsilon_2 M(q_n b) Q_I - a\varepsilon_1 M(q_n a) Q_I) \sqrt{2/\pi} \cos(m\pi z_0 / h) \theta^*(z_0) + Q_2 r_0 M(q_n r_0) + \\ & - Q_0 r_0 M(q_n r_0) \sqrt{2/\pi} \cos(m\pi z_0 / h) \theta^*(z_0) = (q_n^2 + \alpha_m^2) \bar{\Theta}^* + s^\alpha \bar{\Theta}^*. \end{aligned} \quad (3.19)$$

Here

$$\theta^*(z_0) = \begin{cases} 0 & z_0 < 0, \\ 1 & z_0 \geq 0. \end{cases} \quad (3.20)$$

Now, taking inversion of the Laplace transform of Eq.(3.19), one obtain

$$\begin{aligned} \bar{\Theta} = & t^{\alpha-1} E_{\alpha,\alpha} \left(-(q_n^2 + \alpha_m^2) t^\alpha \right) \left\{ (b\varepsilon_2 M(q_n b) Q_l + \right. \\ & - a\varepsilon_1 M(q_n a) Q_l) \sqrt{2/\pi} \cos(m\pi z_0 / h) \theta^*(z_0) + \\ & \left. + Q_2 r_0 M(q_n r_0) - Q_0 r_0 M(q_n r_0) \sqrt{2/\pi} \cos(m\pi z_0 / h) \theta^*(z_0) \right\}. \end{aligned} \tag{3.21}$$

Next, on applying inversion of the Fourier-cosine transform on Eq.(3.21), one obtain

$$\begin{aligned} \bar{\Theta} = & \frac{1}{h} \left\{ t^{\alpha-1} E_{\alpha,\alpha} \left(-(q_n^2 + \alpha_m^2) t^\alpha \right) \left\{ (b\varepsilon_2 M(q_n b) Q_l + \right. \right. \\ & - a\varepsilon_1 M(q_n a) Q_l) \sqrt{2/\pi} \cos(m\pi z_0 / h) \theta^*(z_0) + \\ & \left. \left. + Q_2 r_0 M(q_n r_0) - Q_0 r_0 M(q_n r_0) \sqrt{2/\pi} \cos(m\pi z_0 / h) \theta^*(z_0) \right\} \right\}_{m=0}^{\infty} + \\ & + \sum_{m=1}^{\infty} \left\{ t^{\alpha-1} E_{\alpha,\alpha} \left(-(q_n^2 + \alpha_m^2) t^\alpha \right) \left\{ (b\varepsilon_2 M(q_n b) Q_l + \right. \right. \\ & - a\varepsilon_1 M(q_n a) Q_l) \sqrt{2/\pi} \cos(m\pi z_0 / h) \theta^*(z_0) + Q_2 r_0 M(q_n r_0) + \\ & \left. \left. - Q_0 r_0 M(q_n r_0) \sqrt{2/\pi} \cos(m\pi z_0 / h) \theta^*(z_0) \right\} \times \cos(m\pi z / h) \right\}. \end{aligned} \tag{3.22}$$

Further using inverse of the transform derived by Al-Hajri and Kalla [27] on the above Eq.(3.22), one obtain

$$\begin{aligned} \Theta = & \sum_{n=1}^{\infty} \left[\frac{1}{h} \left\{ t^{\alpha-1} E_{\alpha,\alpha} \left(-(q_n^2 + \alpha_m^2) t^\alpha \right) \left\{ (b\varepsilon_2 M(q_n b) Q_l + \right. \right. \right. \\ & - a\varepsilon_1 M(q_n a) Q_l) \sqrt{2/\pi} \cos(m\pi z_0 / h) \theta^*(z_0) + \\ & \left. \left. + Q_2 r_0 M(q_n r_0) - Q_0 r_0 M(q_n r_0) \sqrt{2/\pi} \cos(m\pi z_0 / h) \theta^*(z_0) \right\} \right\}_{m=0}^{\infty} + \\ & + \sum_{m=1}^{\infty} \left\{ t^{\alpha-1} E_{\alpha,\alpha} \left(-(q_n^2 + \alpha_m^2) t^\alpha \right) \left\{ (b\varepsilon_2 M(q_n b) Q_l + \right. \right. \\ & - a\varepsilon_1 M(q_n a) Q_l) \sqrt{2/\pi} \cos(m\pi z_0 / h) \theta^*(z_0) + \\ & \left. \left. + Q_2 r_0 M(q_n r_0) - Q_0 r_0 M(q_n r_0) \sqrt{2/\pi} \cos(m\pi z_0 / h) \theta^*(z_0) \right\} \times \cos(m\pi z / h) \right\} \times \\ & \times \left\{ \frac{1}{M(q_n)} [B(q_n a, -\varepsilon_1) + B(q_n b, \varepsilon_2)] J_0(q_n r) + \right. \\ & \left. - \frac{1}{M(q_n)} [A(q_n a, -\varepsilon_1) + A(q_n b, \varepsilon_2)] Y_0(q_n r) \right\} \end{aligned} \tag{3.23}$$

where

$$\int_a^b r M(q_n r) M(q_m r) dr = \begin{cases} M(q_n), & m = n, \\ 0, & m \neq n. \end{cases}$$

On reverse variable transformation from Θ to T , the equation of temperature distribution (3.23) becomes

$$\begin{aligned}
T = T_0 + \sum_{n=1}^{\infty} (e^{-\varpi T_0}) & \left[(1 - z^\beta)(k_{m0} - k_{c0}) + k_{c0} \right]^{-1} \left[\frac{I}{h} \left\{ t^{\alpha-1} E_{\alpha,\alpha} \left(-(q_n^2 + \alpha_m^2) t^\alpha \right) \right\} \times \right. \\
& \times \left\{ (b\varepsilon_2 M(q_n b) Q_l - a\varepsilon_1 M(q_n a) Q_l) \times \sqrt{2/\pi} \cos(m\pi z_0 / h) \theta^*(z_0) + Q_2 r_0 M(q_n r_0) + \right. \\
& \left. \left. - Q_0 r_0 M(q_n r_0) \sqrt{2/\pi} \cos(m\pi z_0 / h) \theta^*(z_0) \right\} \right\}_{m=0} + \\
& + \sum_{m=1}^{\infty} \left\{ t^{\alpha-1} E_{\alpha,\alpha} \left(-(q_n^2 + \alpha_m^2) t^\alpha \right) \right\} \left\{ (b\varepsilon_2 M(q_n b) Q_l + \right. \\
& \left. - a\varepsilon_1 M(q_n a) Q_l) \sqrt{2/\pi} \cos(m\pi z_0 / h) \theta^*(z_0) + Q_2 r_0 M(q_n r_0) + \right. \\
& \left. - Q_0 r_0 M(q_n r_0) \sqrt{2/\pi} \cos(m\pi z_0 / h) \theta^*(z_0) \right\} \times \cos(m\pi z / h) \left. \right\} \times \\
& \times \left\{ \frac{I}{M(q_n)} \left[B(q_n a, -\varepsilon_1) + B(q_n b, \varepsilon_2) \right] J_0(q_n r) + \right. \\
& \left. - \frac{I}{M(q_n)} \left[A(q_n a, -\varepsilon_1) + A(q_n b, \varepsilon_2) \right] Y_0(q_n r) \right\}. \tag{3.24}
\end{aligned}$$

4. Thermoelastic equations

The solution of thermoelastic Goodier's potential displacement function obtained by using Eq.(3.24) in Eq.(2.22) as

$$\begin{aligned}
\varphi = \alpha_0 \frac{(1 + \nu)}{(1 - \nu)} & \times \frac{(1 + \cos(m\pi z / h)) z^\beta e^{\chi T}}{u(z) \left(-q_n^2 (1 + \cos(m\pi z / h)) / u(z) \right) + \left[(1 + \cos(m\pi z / h)) / u(z) \right]''} + \\
& + \sum_{n=1}^{\infty} (e^{-\varpi T_0}) \left[(1 - z^\beta)(k_{m0} - k_{c0}) + k_{c0} \right]^{-1} \times T_0 + \sum_{n=1}^{\infty} (e^{-\varpi T_0}) \left[(1 - z^\beta)(k_{m0} - k_{c0}) + \right. \\
& \left. + k_{c0} \right]^{-1} + \left(\sum_{m=1}^{\infty} \left[\frac{I}{h} \left\{ t^{\alpha-1} E_{\alpha,\alpha} \left(-(q_n^2 + \alpha_m^2) t^\alpha \right) \right\} \left\{ (b\varepsilon_2 M(q_n b) Q_l - a\varepsilon_1 M(q_n a) Q_l) \right\} \times \right. \right. \\
& \times \sqrt{2/\pi} \cos(m\pi z_0 / h) \theta^*(z_0) + Q_2 r_0 M(q_n r_0) + \\
& \left. \left. - Q_0 r_0 M(q_n r_0) \sqrt{2/\pi} \cos(m\pi z_0 / h) \theta^*(z_0) \right\} \right\}_{m=0} + \\
& + \sum_{m=1}^{\infty} \left\{ t^{\alpha-1} E_{\alpha,\alpha} \left(-(q_n^2 + \alpha_m^2) t^\alpha \right) \right\} \left\{ (b\varepsilon_2 M(q_n b) Q_l + \right. \\
& \left. - a\varepsilon_1 M(q_n a) Q_l) \sqrt{2/\pi} \cos(m\pi z_0 / h) \theta^*(z_0) + Q_2 r_0 M(q_n r_0) + \right. \\
& \left. - Q_0 r_0 M(q_n r_0) \sqrt{2/\pi} \cos(m\pi z_0 / h) \theta^*(z_0) \right\} \times \cos(m\pi z / h) \left. \right\} \times \tag{4.1}
\end{aligned}$$

$$\times \left\{ \frac{I}{M(q_n)} \left[B(q_n a, -\varepsilon_1) + B(q_n b, \varepsilon_2) \right] J_0(q_n r) + \right. \\ \left. - \frac{I}{M(q_n)} \left[A(q_n a, -\varepsilon_1) + A(q_n b, \varepsilon_2) \right] Y_0(q_n r) \right\} \quad (\text{cont.4.1})$$

Let the Michell's function as given below satisfy the condition governed by Eq.(2.26)

$$M = \sum_{n=1}^{\infty} \sum_{m=1}^{\infty} \cos(\Omega z) \psi_1^n t^{n-\alpha} E_{1,n-\alpha+1}(\psi_1 t) \left[C_m J_0(q_n r) + D_m r Y_0(q_n r) \right] \quad (4.2)$$

where C_m and D_m are constants.

Next, on substitution Eqs (4.1) and (4.2) in (2.24)-(2.25) the displacement components are obtained as

$$u = \sum_{n=1}^{\infty} \sum_{m=1}^{\infty} \left[\frac{\partial \phi}{\partial r} - (\Omega \sin(\Omega z)) \psi_1^n t^{n-\alpha} E_{1,n-\alpha+1}(\psi_1 t) \times \right. \\ \left. \times \left[C_m q_n J_1(q_n r) + D_m q_n r Y_1(q_n r) - D_m Y_0(q_n r) \right] \right], \quad (4.3)$$

$$w = \sum_{n=1}^{\infty} \sum_{m=1}^{\infty} \left\{ \frac{\partial \phi}{\partial z} + 2(1-\nu)(\cos(\Omega z)) \psi_1^n t^{n-\alpha} E_{1,n-\alpha+1}(\psi_1 t) \times \right. \\ \left. \times \left[-C_m q_n^2 J_0(q_n r) + D_m Y_0(q_n r) \right] \left[\frac{1}{r} - q_n r \right] \right\} + \\ + (1-2\nu) \left[-\Omega^2 \cos \Omega z \right] \psi_1^n t^{n-\alpha} E_{1,n-\alpha+1}(\psi_1 t) \times \left[C_m J_0(q_n r) + D_m r Y_0(q_n r) \right]. \quad (4.4)$$

The stress components from (2.27)-(2.30) for both the homogeneous and non-homogeneous case can be obtained using (4.3)-(4.4) by setting $(\beta = \varpi = \chi = 0)$ and $(\beta \neq \varpi \neq \chi \neq 0)$, respectively. Also, the values of constant are calculated by using traction free boundaries. Mathematica is utilized for all numerical computations.

5. Numerical calculations

For the purpose of numerical analysis alumina is set as the ceramic and nickel as metal to form functionally graded metal-ceramic base is considered.

Where non-dimensional variables are as:

$$T^* = \frac{T}{T_R}, \quad \eta = \frac{r}{a}, \quad \zeta = \frac{z}{a}, \quad t^* = \frac{\kappa t}{a^2}, \quad u^* = \frac{(1-\nu)u}{(1+\nu)\alpha_0 T_0 a}, \quad w^* = \frac{(1-\nu)w}{(1+\nu)\alpha_0 T_0 a},$$

$$\sigma_{rr}^* = \frac{\sigma_{rr}}{G_0 \alpha_0 T_0}, \quad \sigma_{\theta\theta}^* = \frac{\sigma_{\theta\theta}}{G_0 \alpha_0 T_0}, \quad \sigma_{zz}^* = \frac{\sigma_{zz}}{G_0 \alpha_0 T_0}, \quad \sigma_{rz}^* = \frac{\sigma_{rz}}{G_0 \alpha_0 T_0}.$$

The dimensions used during the numerical calculation are as follows: inner radius of a cylinder $a = 1\text{ cm}$, outer radius of a cylinder $b = 2\text{ cm}$, $h = 1\text{ cm}$, $T_0 = 320^\circ\text{ K}$.

The other related values are as taken:

For Alumina (Ceramic):

thermal conductivity $k = 0.282\text{ W/cmK}$,

specific heat capacity $C = 0.78\text{ J/gK}$,

shear modulus $G = 12.4 \times 10^6\text{ N/cm}^2$,

coefficient of linear thermal expansion $\alpha = 5.4 \times 10^{-6}\text{ /K}$,

Poisson's ratio $\nu = 0.23$.

For Nickel (Metal):

thermal conductivity $k = 0.901\text{ W/cmK}$,

specific heat capacity $C = 0.44\text{ J/gK}$,

shear modulus $G = 7.6 \times 10^6\text{ N/cm}^2$,

coefficient of linear thermal expansion $\alpha = 14 \times 10^{-6}\text{ /K}$,

Poisson's ratio $\nu = 0.31$.

5.1. Analysis of numerical results

MATHEMATICA software is used for the purpose of numerical analysis of temperature distribution, radial stress distribution, tangential stress distribution, axial stress and shear stress distribution for different values of the fractional-order parameter $\alpha = 0.5$, $\alpha = 1$, $\alpha = 1.5$, $\alpha = 2$ (depicting weak, normal and strong conductivity) for the case of the functionally graded thermosensitive hollow cylinder.

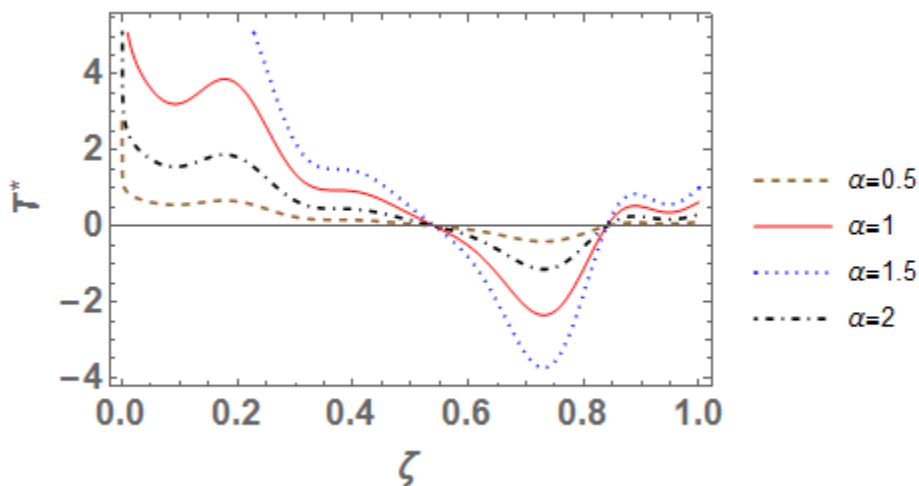


Fig.2a. Dimensionless temperature distribution function along the axial direction in the homogeneous cylinder.

Figures 2a and 2b present the distribution of dimensionless temperature T^* along the dimensionless axial direction ζ in both homogeneous and non-homogeneous cylinder for different values of the fractional order parameter α by fixing $\eta = 1.5$. It is observed that due to prescribed varying heat source at the lower surface, the same temperature is noted in both the homogeneous and non-homogeneous cases. Further, the temperature distribution slowly decreases towards the upper surface by somehow showing sinusoidal type behavior in the non-homogenous case. Also, it is observed that the speed of thermal signals propagation vary

directly proportional to the values of the fractional-order parameter α in both the cases. For non-homogeneous case the magnitude of temperature distribution is found low as compared to the homogeneous case.

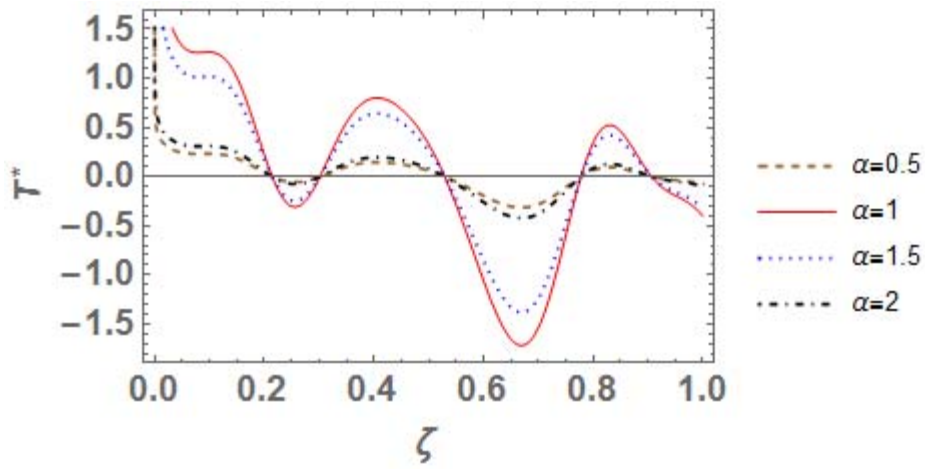


Fig.2b. Dimensionless temperature distribution function along the axial direction in the non-homogeneous cylinder.

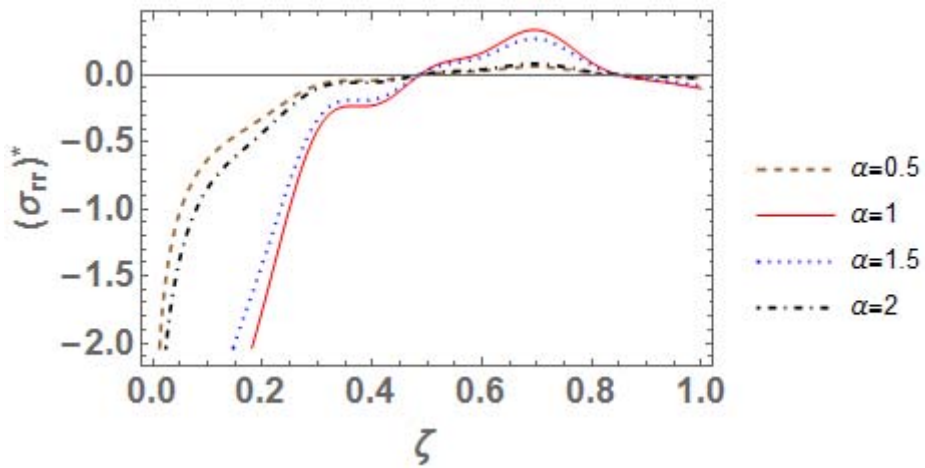


Fig.3a. Dimensionless radial stress distribution along the axial direction in the homogeneous cylinder.

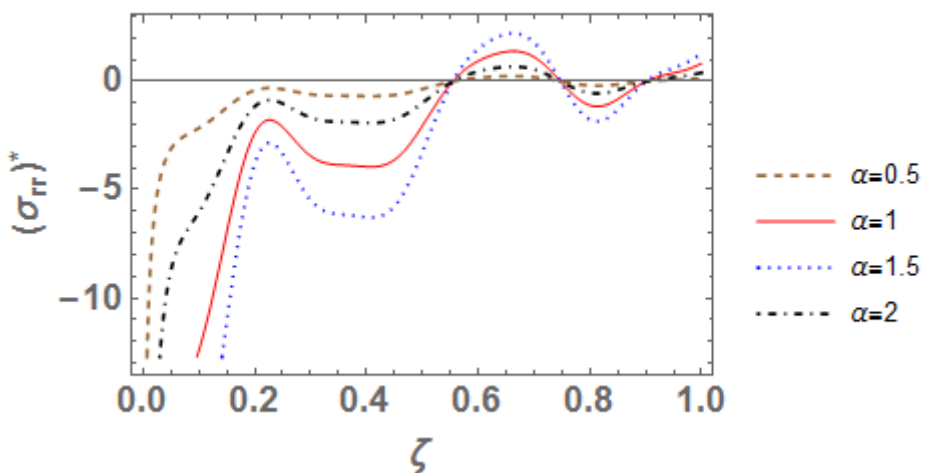


Fig.3b. Dimensionless radial stress distribution along the axial direction in the non-homogeneous cylinder.

Figures 3a and 3b present the distribution of dimensionless radial stress σ_{rr}^* along the dimensionless axial direction ζ in both the homogeneous and non-homogeneous cylinder for different values of the fractional order parameter α by fixing $\eta=1.5$. It is observed that stress distribution gradually increases on going from the lower to the upper surface for different fraction parameters in both the homogeneous and non-homogeneous cases. Also the effect of varying heat source on the curved surface can be noted here. Further, stress distribution slowly decreases towards the upper surface and the impact of stress propagation is found varying inversely proportional to the different values of the fractional-order parameter α in both the cases.

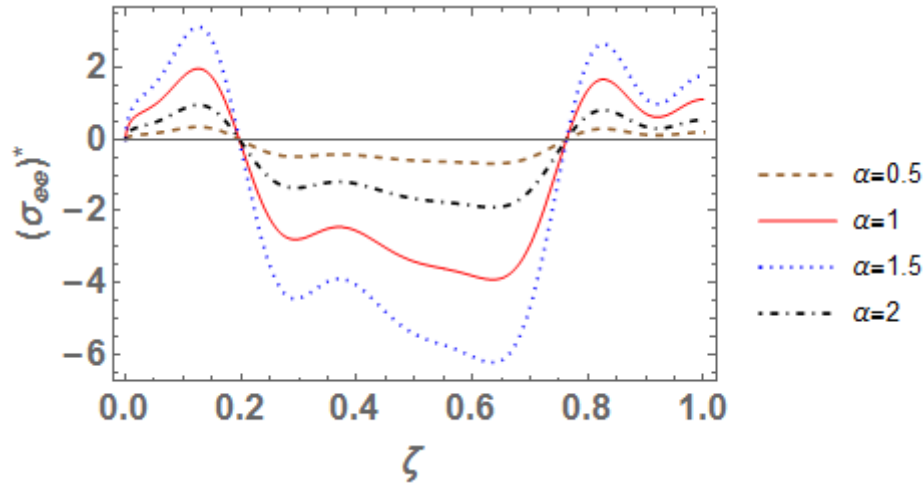


Fig.4a. Dimensionless tangential stress distribution along the axial direction in the homogeneous cylinder.

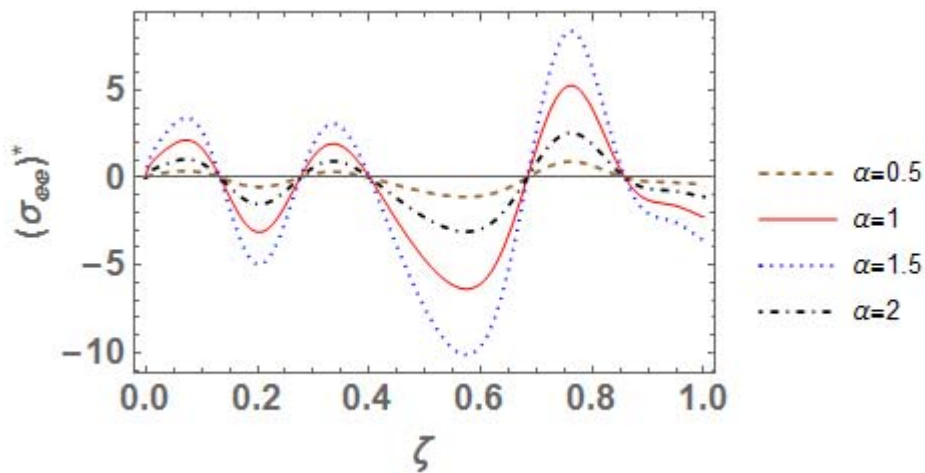


Fig.4b. Dimensionless tangential stress distribution along the axial direction in the non-homogeneous cylinder.

Figures 4a and 4b present the distribution of dimensionless tangential stress $\sigma_{\theta\theta}^*$ along the dimensionless axial direction ζ in both the homogeneous and non-homogeneous cylinder for different values of the fractional order parameter α by fixing $\eta=1.5$. For the homogeneous case, the radial stress distribution shows compressive behavior while in the non-homogeneous case the radial stress has a sinusoidal nature throughout the thickness. The magnitude of stress is found to be decreasing in between the upper and lower surface for different values of the fractional parameter.

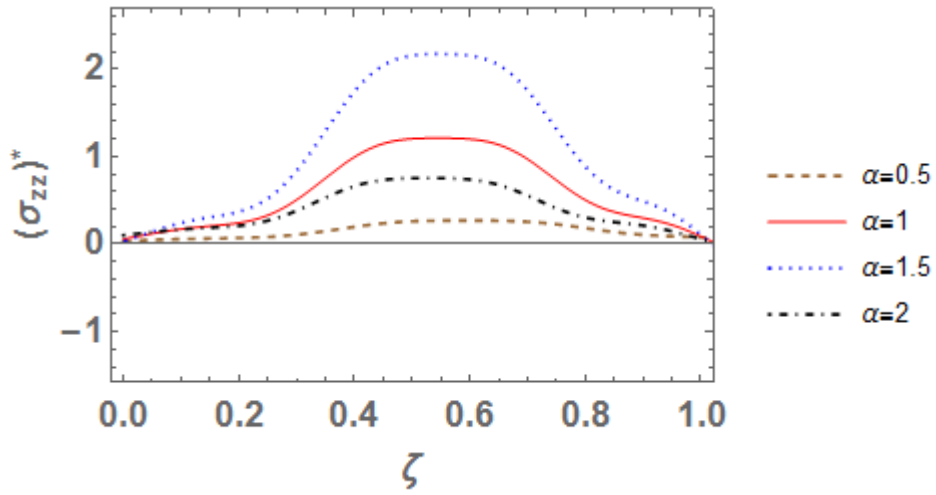


Fig.5a. Dimensionless axial stress distribution along the axial direction in the homogeneous cylinder.

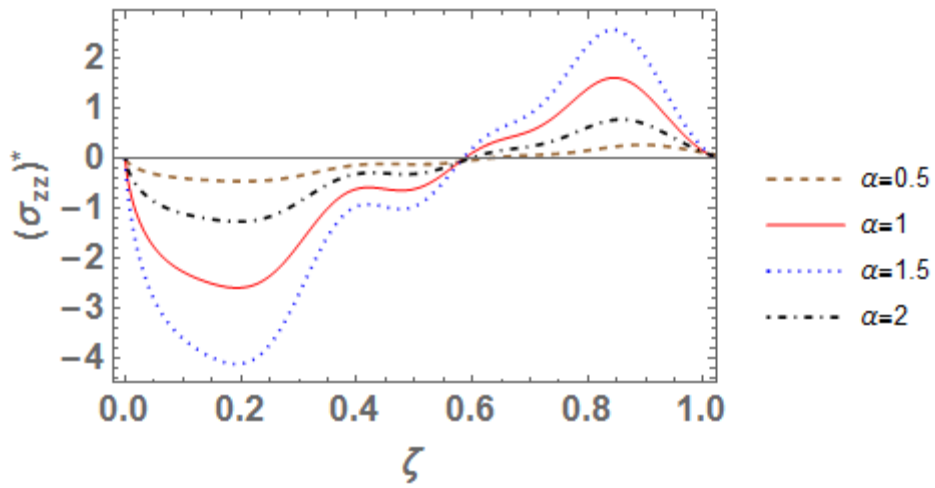


Fig.5b. Dimensionless axial stress distribution along the axial direction in the non-homogeneous cylinder.

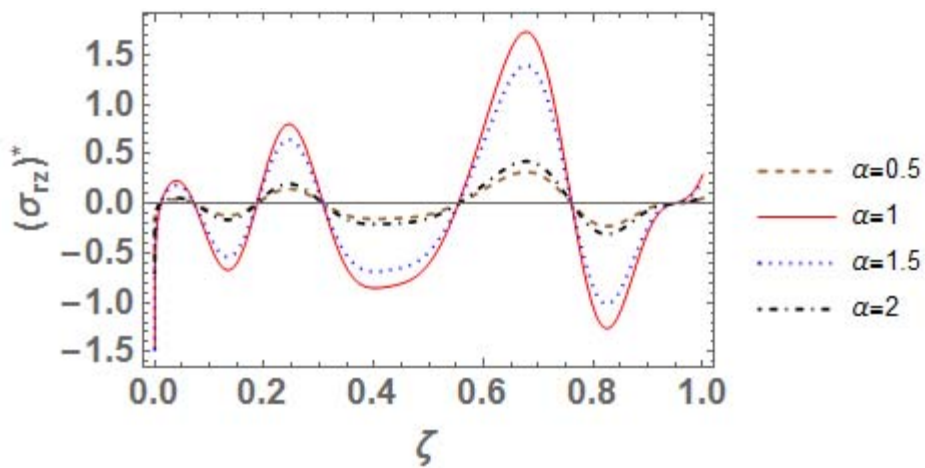


Fig.6a. Dimensionless shear stress distribution along the axial direction in the homogeneous cylinder.

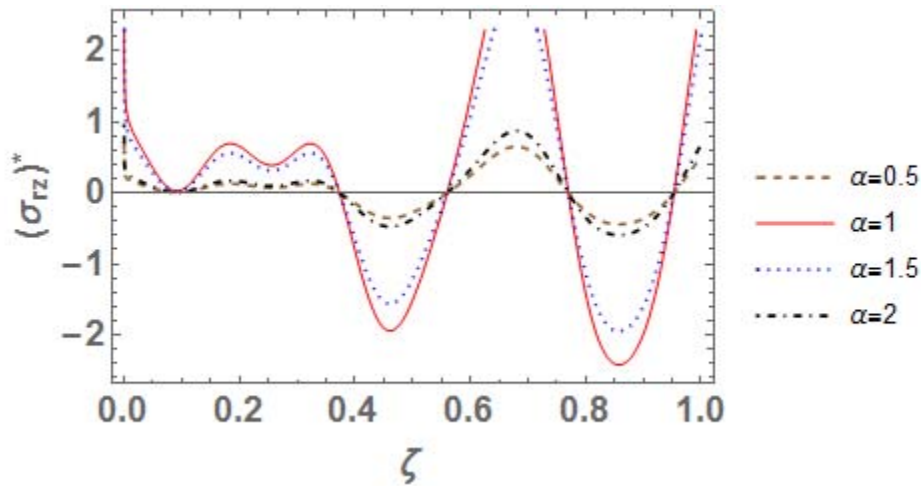


Fig.6b. Dimensionless shear stress distribution along the axial direction in the non-homogeneous cylinder.

Figures 5a and 5b present the distribution of dimensionless axial stress σ_{zz}^* along the dimensionless axial direction ζ in both the homogeneous and non-homogeneous cylinder for different values of the fractional order parameter α by fixing $\eta=1.5$. From the plotting it is noted that for both the homogeneous and non-homogeneous cases the nature of the graph is sinusoidal. Also, stress behavior is compressive in the homogeneous case throughout the functionally graded cylinder. Its magnitude increases towards the central region and starts decreasing towards the upper surface. In the non-homogeneous case stresses are compressive in the range $0 < \zeta < 0.65$ and tensile in the range $0.65 < \zeta < 1$. Further, mathematical boundary condition defined in Eq.(3.31) completely matches the above graphical plotting.

Figures 6a and 6b present the distribution of dimensionless shear stress σ_{rz}^* along the dimensionless axial direction ζ in both the homogeneous and non-homogeneous cylinder for different values of the fractional order parameter α by fixing $\eta=1.5$. The plotting shows sinusoidal type behavior in both the homogeneous and non-homogeneous cases. Also, the magnitude of stress distribution is found more in the non-homogeneous case as compared to the homogeneous case. Further, the different values of the fractional parameter significantly affect the variation of stresses on going from the lower to the upper surface.

6. Conclusion

In the article, a thermoelastic problem of a thick hollow cylinder under time-fractional order heat conduction equation is studied under the influence of thermosensitive material properties. The integral transform method is applied to analyze the thermal behavior of the cylinder with internal heat generation subjected to convection boundaries on the curved surface as well as heat flux at the lower surface. All material properties except Poisson's ratio were assumed to depend on both temperature and axial direction. For the numerical analysis thermo-mechanical properties of alumina and nickel at room temperature were utilized for both the homogeneous and non-homogeneous case. From the numerical analysis for the functionally graded thermosensitive thick hollow cylinder it is concluded that the speed of wave propagation is influenced by taking different values of the fractional parameter α in the both homogeneous and non-homogeneous cases as shown in Figs 2-6. Convection type boundary condition following Newton's law of cooling on curved surfaces and heat flux at the lower surface also affect the flow of temperature and stresses distribution on moving from the lower to the upper surface. Hence, all the above discussed factors can be useful for designing new materials and is applicable to real life situations. Hence we say that the functionally graded thermosensitive thick hollow cylinder with internal heat generation in the context of fractional order

theory approach predicts very useful structural effect on design of different models in engineering and applied sciences. Hence, we conclude that the above study is useful for the design of new materials.

Acknowledgment

The author gratefully acknowledges the discussion with the Editor-in-Chief, Prof. Pawel Jurczak, and Editorial Staff of International Journal of Applied Mechanics and Engineering to bring this manuscript in the present form which improves the quality of work a lot.

Nomenclature

- $c(z, T)$ – specific heat capacity
 $e_{rr}, e_{\theta\theta}, e_{zz}$ – strain components
 $G_0 z^\beta e^{\sigma T}$ – shear modulus
 $k(z, T)$ – thermal conductivity
 M – Michell's function
 $T(r, z, t)$ – temperature distribution at any time t
 T_0 – surrounding medium temperature
 u – displacement components along radial direction
 w – displacement components along axial direction
 $r = a$ – inner radius of cylinder
 $r = b$ – outer radius of cylinder
 z – thickness of cylinder
 α – time-fractional order derivative
 $\alpha_0 z^\beta e^{\lambda T}$ – thermal expansion coefficient
 $\varepsilon_1, \varepsilon_2$ – coefficients of heat transfer
 $\lambda_0 z^\beta e^{\sigma T}$ – Lamé's constant
 $\mu_0 z^\beta e^{\sigma T}$ – Lamé's constant
 φ – Goodier's displacement potential
 ϕ, ψ – Boussinesq harmonic functions

References

- [1] Povstenko Y.Z. (2005): *Fractional heat conduction equation and associated thermal stresses.*– Journal of Thermal Stresses, vol.28, pp.83-102.
- [2] Povstenko Y. Z. (2010): *Fractional radial heat conduction in an infinite medium with a cylindrical cavity and associated thermal stresses.*– Mech. Res. Commun., vol.37, pp.436-440.
- [3] Povstenko Y.Z. (2011): *Non-axisymmetric solutions to time-fractional diffusion-wave equation in an infinite cylinder.*– Fract. Calc. Appl. Anal., vol.14, No.3, pp.418-435.
- [4] Povstenko Y.Z. (2011): *Solutions to time-fractional diffusion-wave equation in cylindrical coordinates.*– Advances in Differential Equations, vol.2011, Article ID.930297, p.14, doi:10.1155/2011/930297.
- [5] Povstenko Y.Z. (2011): *Non-axisymmetric solutions to time-fractional heat conduction equation in a half-space in cylindrical coordinates.*– Math. Methods Phys.-Mech. Fields, vol.54, No.1, pp.212-219.
- [6] Povstenko Y.Z. (2015): *Fractional thermoelasticity, solid mechanics and its application.*– Springer, vol. 219, p.293, <https://doi.org/10.1007/978-3-319-15335-3>.

- [7] Popovich V.S. and Garmatii G.Yu. (1993): *Analytic-numerical methods of constructing solutions of heat-conduction problems for thermosensitive bodies with convective heat transfer.*– Ukrainian Academy of Sciences, Pidstrigach Institute for Applied Problems of Mechanics and Mathematics, L'viv, Preprint, pp.13-93.
- [8] Popovich V.S. and Fedai B.N. (1997): *The axisymmetric problem of thermoelasticity of a multilayer thermosensitive tube.*– Journal of Mathematical Sciences, vol.86, No.2, pp.2605-2610.
- [9] Popovich V.S. and Makhorkin I.M. 1998: *On the solution of heat-conduction problems for thermosensitive bodies.*– Journal of Mathematical Sciences, vol.88, No.3, pp.352-359
- [10] Kushnir R. and Popovych V.S. (2009): *Thermoelasticity of Thermosensitive Solids (in Ukrainien).*– SPOLOM, Lviv, p.419.
- [11] Kushnir R. and Popovych V.S. (2011): *Heat conduction problems of thermosensitive solids under complex heat exchange.*– Heat Conduction - Basic Research, INTECH., pp.131-154, DOI: 10.5772/27970.
- [12] Popovych V.S., Vovk O.M. and Yu H. (2012): *Investigation of the static thermoelastic state of a thermosensitive hollow cylinder under convective-radiant heat exchange with environment.*– Journal of Mathematical Sciences, vol.187, No.6, pp.726-736.
- [13] Guo Li-C. and Noda N. (2010): *An analytical method for thermal stresses of a functionally graded material cylindrical shell under a thermal shock.*– Acta Mechanica, vol.214, pp.71-78.
- [14] Cheng Z.Q. and Batra R.C. (2000): *Deflection relationships between the homogenous Kirchhoff plate theory and different functionally graded plate theories.*– Arch. Mech., vol.52, No.1, pp.143-158.
- [15] Cheng Z.Q. and Batra R.C. (2000): *Three-dimensional thermoelastic deformations of a functionally graded elliptic plate.*– Composites: Part B, vol.31, pp.97-106.
- [16] Kamdi D. B. and Lamba N. K. (2016): *Thermoelastic analysis of functionally graded hollow cylinder subjected to uniform temperature field.*– Journal of Applied and Computational Mechanics, vol.2, No.2, pp.118-127.
- [17] Rajneesh K., Manthena V.R., Lamba N.K. and Kedar G.D. (2017): *Generalized thermoelastic axisymmetric deformation problem in a thick circular plate with dual phase lags and two temperatures.*– Materials Physics and Mechanics, vol.32, No.2, pp.123-132.
- [18] Rajneesh K. and Navneet K. (2020): *Analysis of nano-scale beam by eigenvalue approach in modified couple stress theory with thermoelastic diffusion.*– Southeast Asian Bulletin of Mathematics, vol.44, pp.515-532.
- [19] Navneet K. and Kamdi D.B. (2020): *Thermal behavior of a finite hollow cylinder in context of fractional thermoelasticity with convection boundary conditions.*– Journal of Thermal Stresses, vol.43, No.9, pp.1189-1204.
- [20] Lamba N.K. and Deshmukh K.C. (2020): *Hygrothermoelastic response of a finite solid circular cylinder.*– Multidiscipline Modeling in Materials and Structures, vol.16, No.1, pp.37-52.
- [21] Kamdi D.B. and Navneet K. (2020): *Thermal behaviour of an annular fin in context of fractional thermoelasticity with convection boundary conditions.*– Annals of Faculty Engineering Hunedoara – International Journal of Engineering, vol.18, No.4, p.9.
- [22] Thakare S. and Warbhe M. (2020): *Analysis of time-fractional heat transfer and its thermal deflection in a circular plate by a moving heat source.*– International Journal of Applied Mechanics and Engineering, vol.25, No.3, pp.158-168.
- [23] Shivcharan T. and Warbhe M.S. (2021): *Time fractional heat transfer analysis in thermally sensitive functionally graded thick hollow cylinder with internal heat source and its thermal stresses.*– J. Phys.: Conf. Ser., vol.1913, No.1, pp.1-13.
- [24] Shivcharan T., Warbhe M.S. and Navneet K. (2020): *Time fractional heat transfer analysis in non-homogeneous thick hollow cylinder with internal heat generation and its thermal stresses.*– International Journal of Thermodynamics, vol. 23, No.4, pp.281-302.
- [25] Hata T. (1982): *Thermal stresses in a nonhomogeneous thick plate under steady distribution of temperature.*– Journal Thermal Stresses, vol. 5, pp.1-11.
- [26] Noda N. (1986): *Thermal stresses in materials with temperature dependent properties.*– Thermal Stresses I, Taylor & Francis, North Holland, Amsterdam, pp.391-483.
- [27] Al-Hajri M. and Kalla S.L. (2004): *On an integral transform involving Bessel functions* - Proceedings of the international conference on Mathematics and its applications, Kuwait, April 5-7.

Received: July 14, 2021

Revised: November 18, 2021